4 Transmitting Transducer and the Sound Generation Process

In this Chapter we will discuss models of the ultrasonic transducer as a transmitting device that converts electrical energy into acoustic energy. We will also combine the models of the pulser and cabling from Chapters 2 and 3 with the transducer model of this Chapter to describe a model of the entire sound generation process.

4.1 Transducer Modeling

An ultrasonic transducer is normally based on a piezoelectric material that has the ability to convert electrical energy at its electrical port into acoustic energy (motion) at its acoustic port and, conversely, to also convert acoustic energy back into electrical energy. Thus a piezoelectric ultrasonic transducer can act as both a transmitter and receiver of sound. In this Chapter we will examine the transducer in its role as a transmitter. By treating the coupled electromagnetic and elastic fields contained in the transducer as those of a piezoelectric medium and considering the fields at the two transducer ports as purely electrical fields and acoustic fields that arise from those internal piezoelectric interactions, one can define a reciprocity relationship between the fields at the two ports in the form [4.1-4.3]

$$\int_{S_c} \left(\mathbf{E}^{(2)} \times \mathbf{H}^{(1)} - \mathbf{E}^{(1)} \times \mathbf{H}^{(2)} \right) \cdot \mathbf{n} \, dS = \int_{S} \left(p^{(1)} \mathbf{v}^{(2)} - p^{(2)} \mathbf{v}^{(1)} \right) \cdot \mathbf{n} \, dS, \tag{4.1}$$

where $(\mathbf{E}, \mathbf{H})$ are the electrical and magnetic fields at the transducer's electrical port (over area S_c) and $(p, \mathbf{v})$ are the pressure and velocity fields at the acoustic port (over area S), and $\mathbf{n}$ is the unit normal pointing outwards from each port (see Fig. 4.1). Only the pressure appears on the right side of Eq. (4.1) since for an immersion transducer this is the only component of the stress tensor that can exist for a fluid. Even for a contact transducer, however, there is normally a thin fluid couplant layer between the transducer

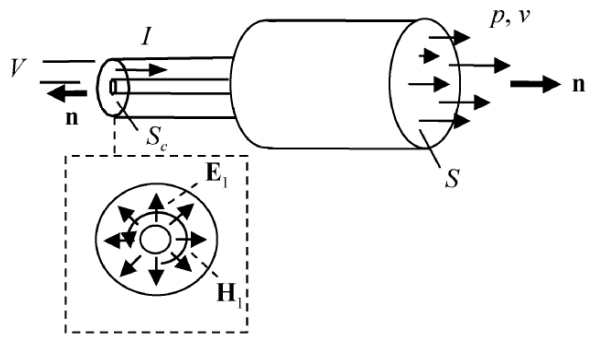

Fig. 4.1. The electrical and magnetic fields at a transducer's electrical port and the corresponding voltage and current flowing into that port. At the acoustic port distributed pressure and velocity fields are generated, as shown.

and the solid component so that in contact testing again only a pressure exists at the transducer face. The superscripts (1) and (2) indicate these fields for two different states (i.e. under two different sets of driving and termination conditions). If we assume that the electrical and magnetic fields at the electrical port are in the form of TEM waves, as done for the cable in the previous Chapter, then we have [4.3]

$$V^{(1)}I^{(2)} - V^{(2)}I^{(1)} = -\int_S \left(p^{(2)}\mathbf{v}^{(1)} - p^{(1)}\mathbf{v}^{(2)} \right) \cdot \mathbf{n}\, dS, \tag{4.2}$$

where V and I are the voltage and current flowing into the electrical port, as shown in Fig. 4.1. At the acoustic port, we will assume the transducer acts as a piston transducer, i.e. the velocity is constant over the area S. This is an assumption frequently used to model ultrasonic transducers and is one we will adopt here. In that case, the right side of Eq.(4.2) can be expressed in terms of the two quantities, F and v, where

$$\begin{aligned} F(\omega) &= \int_p p(\mathbf{x},\omega)\, dS(\mathbf{x}) \\ v(\omega) &= \mathbf{v}(\omega) \cdot \mathbf{n} \end{aligned} \tag{4.3}$$

so that F is the compressive force acting at the transducer face and v is the uniform outward normal velocity on this face. In this case Eq. (4.2) becomes

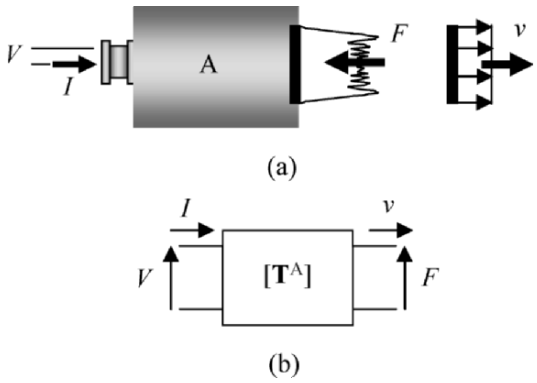

Fig. 4.2. (a) An ultrasonic transducer represented as a device that converts voltage and current into force and velocity and **(b)** its corresponding two port system representation. The pressure distribution over the acoustic port that generates the force F is generally non-uniform, as shown. However, we assume the velocity distribution at the acoustic port is uniform as shown, i.e. the transducer acts as a piston.

$$V^{(1)}I^{(2)} - V^{(2)}I^{(1)} = F^{(1)}v^{(2)} - F^{(2)}v^{(1)}, \tag{4.4}$$

which is the reciprocity relation in terms of "lumped" parameters. Even if the transducer does not act as a piston, it is possible to use Eq. (4.4). The details can be found in [4.3] but we will not discuss that generalization here. In terms of these parameters, therefore, we can consider a transducer as a two port device that converts voltage and current into force and velocity, as shown in Fig. 4.2. If the reciprocity relation Eq. (4.4) is satisfied for all states then this two port system can be written in terms of a reciprocal transfer matrix $\left[\mathbf{T}^A\right]$, where

$$\begin{Bmatrix} V \\ I \end{Bmatrix} = \begin{bmatrix} T_{11}^A & T_{12}^A \\ T_{21}^A & T_{22}^A \end{bmatrix} \begin{Bmatrix} F \\ v \end{Bmatrix} \quad , \quad \det\left[\mathbf{T}^A\right] = 1. \tag{4.5}$$

By modeling the fields in the transducer as 1-D fields, Sittig [4.4], [4.5] developed an explicit expression for the transfer matrix components that describe a compressional wave transducer. In the Sittig model, the

transfer matrix of a transducer A, $\left[\mathbf{T}^A\right]$, can be written as a product of two 2x2 transfer matrices, $\left[\mathbf{T}_e^A\right]$,$\left[\mathbf{T}_a^A\right]$, as $\left[\mathbf{T}^A\right]=\left[\mathbf{T}_e^A\right]\left[\mathbf{T}_a^A\right]$, where

$$\begin{aligned}\left[\mathbf{T}_e^A\right]&=\begin{bmatrix}1/n & n/i\omega C_o\\ -i\omega C_o & 0\end{bmatrix}\\ \left[\mathbf{T}_a^A\right]&=\frac{1}{Z_b^a-iZ_0^a\tan\left(kd/2\right)}\\ &\cdot\begin{bmatrix}Z_b^a+iZ_0^a\cot\left(kd\right) & \left(Z_0^a\right)^2+iZ_0^aZ_b^a\cot\left(kd\right)\\ 1 & Z_b^a-2iZ_0^a\tan\left(kd/2\right)\end{bmatrix}.\end{aligned} \tag{4.6}$$

The multiple parameters appearing in this model are as follows. The parameter k is the wave number for the piezoelectric plate, $k=\omega/v_0$, where v_0 is the wave speed of compressional waves in the piezoelectric plate given by $v_0=\sqrt{c_{33}^D/\rho_P}$ in terms of the elastic constant of the plate, c_{33}^D, at constant electric flux density, and ρ_P, the density of the plate. The constant $n=h_{33}C_0$ is given in terms of h_{33}, a piezoelectric stiffness constant for the plate, and C_0, the clamped capacitance of the plate, which is given by $C_0=S/\beta_{33}^S d$, where S is the area of the piezoelectric plate, β_{33}^S is the dielectric impermeability of the plate at constant strain, and d is the plate thickness. The quantity $Z_0^a=\rho_P v_0 S$ is the plane wave acoustic impedance of the piezoelectric plate, while $Z_b^a\left(\omega\right)$is the corresponding acoustic impedance of the backing (which is a function of frequency since the backing normally consists of one or more layers and is highly attenuating).

It can be seen from Eq. (4.6) that in order to use the Sittig model one must know in considerable detail the internal material and geometry parameters of the transducer. When designing and manufacturing transducers, such details are known explicitly but it is not possible to obtain such detailed knowledge of transducers that are purchased commercially. Thus, one must rely instead on experimental means to determine the transfer matrix of the transducer. Unfortunately, at present a practical experimental method does not exist that can determine the complete transfer matrix of an ultrasonic transducer. The problem lies in the fact that it is difficult to enforce different known termination conditions at the acoustic port (as was done in the cable case for one of the electrical

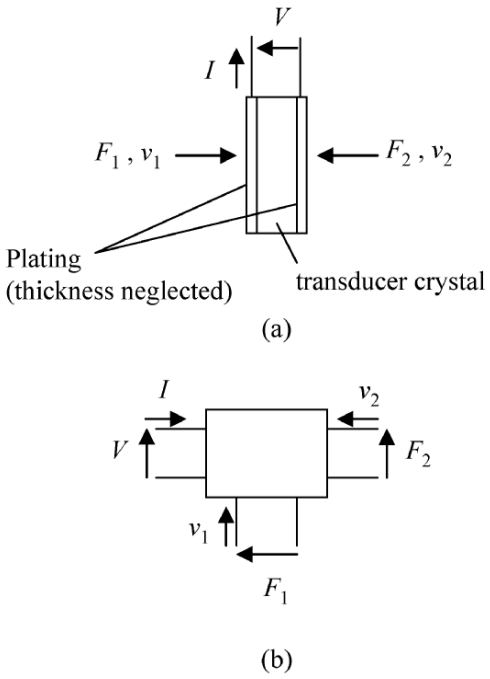

Fig. 4.3. (a) A 1-D model of the electrical and acoustic parameters for a plated piezoelectric crystal and **(b)** its representation as a three port system.

ports of the cable). Also, while it is easy to measure the voltage and current at the electrical port of the transducer it is more difficult to measure the force and velocity parameters at the acoustic port without investing in expensive equipment. Fortunately, as we will show later, we can characterize the role of the transducer in an ultrasonic measurement setup in terms of only two parameters that are related to the transducer's transfer matrix. These two parameters are the transducer's sensitivity and its equivalent electrical impedance. We will also show that it is possible to determine the sensitivity and impedance with purely electrical measurements at the transducer's electrical port. Thus, we can bypass the need to have the full set of transfer matrix components for characterizing the transducer.

In designing ultrasonic transducers, many designers find it convenient to use a three port model instead of the two port Sittig model. The Mason model and the KLM model are two models of this type that are commonly used in practice [4.6],[4.7]. Like the Sittig model, both models

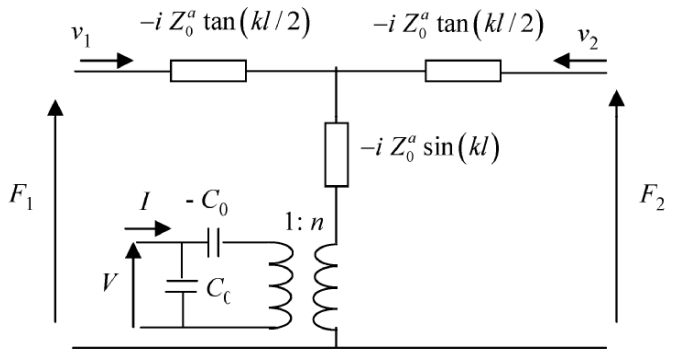

Fig. 4.4. The Mason equivalent circuit model of the three port system defined by Eq. (4.7).

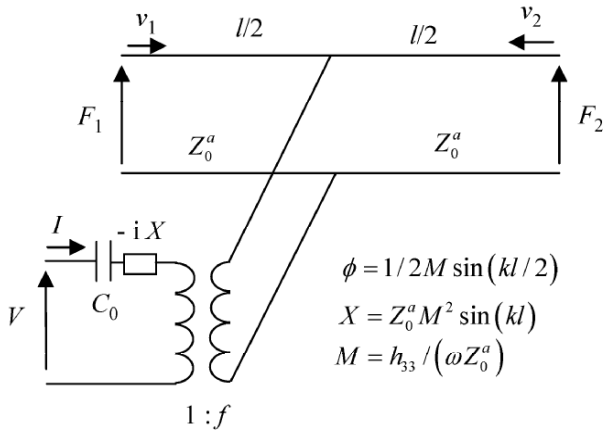

Fig. 4.5. The KLM equivalent circuit model for the three port system defined by Eq. (4.7).

treat the transducer as a plated piezoelectric element where 1-D electrical and mechanical fields are present, as shown in Fig. 4.3. The electrical port is where electrical connections are made to the plated faces of the piezoelectric plate while the two acoustic ports are the two faces of the plate (Fig. 4.3). The electrical and mechanical lumped parameters for this three port model can be shown to satisfy the relations [4.8]

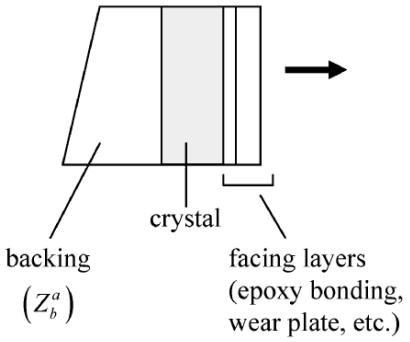

Fig. 4.6. Construction of a typical commercial transducer showing the crystal backing and one or more facing acoustic layers at the transducer acoustic output port.

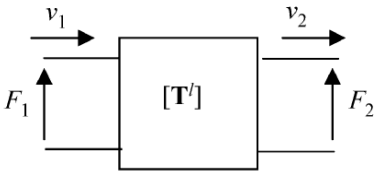

Fig. 4.7. The acoustic two port system model of an acoustic layer.

$$\begin{Bmatrix} F_1 \\ F_2 \\ V \end{Bmatrix} = i \begin{bmatrix} Z_0^a \cot(kl) & Z_0^a / \sin(kl) & h_{33}/\omega \\ Z_0^a / \sin(kl) & Z_0^a \cot(kl) & h_{33}/\omega \\ h_{33}/\omega & h_{33}/\omega & 1/\omega C_0 \end{bmatrix} \begin{Bmatrix} v_1 \\ v_2 \\ I \end{Bmatrix}, \tag{4.7}$$

which can be seen to be given in the form of a 3x3 impedance matrix. Note that in Eq. (4.7) the velocities are assumed to be flowing into the transducer at the acoustic ports. This convention is opposite to what is assumed (at the acoustic output port) of a transfer matrix model (see Fig. 4.2 (b)). If the material backing on the piezoelectric element is specified as a given acoustic impedance, $Z_b^a(\omega)$, as done for the Sittig model, then this three port model reduces to a two port model. The Sittig model is just a transfer matrix representation of the resulting two port system. In contrast, the Mason and KLM models are just equivalent circuit

representations of the three port system described by Eq. (4.7) where the acoustic impedance of the backing of the piezoelectric element is not specified. Figure 4.4 shows a schematic of the Mason equivalent circuit model and Fig. 4.5 shows the KLM equivalent circuit.

The Sittig model is a particularly useful model to use to consider additional acoustic layers in the transducer model at the transducer output port. Such layers are normally present in the form of wear plates to protect the piezoelectric element or impedance matching plates (Fig. 4.6) and can be represented as acoustic two port systems (Fig. 4.7). The transfer matrix $\left[\mathbf{T}^{l}\right]$ for an acoustic layer containing 1-D propagating compressional waves is given by

$$\begin{Bmatrix} F_1 \\ v_1 \end{Bmatrix} = \begin{bmatrix} \cos\left(k_a l_a\right) & -iZ_0^a \sin\left(k_a l_a\right) \\ -i\sin\left(k_a l_a\right)/Z_0^a & \cos\left(k_a l_a\right) \end{bmatrix} \begin{Bmatrix} F_2 \\ v_2 \end{Bmatrix}, \tag{4.8}$$

where $k_a = \omega/c$ is the wave number for waves traveling in the layer with compressional wave speed, c, l_a is the layer thickness, and $Z_0^a = \rho c S$ is the acoustic impedance of the layer, with ρ the density of the layer and S is the cross-sectional area. Note that this transfer matrix has exactly the same form as the matrix obtained for a cable, so this matrix is the acoustic analog of that electrical model. A transducer containing such an acoustic layer can be joined with the Sittig model by simply multiplying that model by an additional acoustic transfer matrix so that the entire transfer matrix for the transducer, $[\mathbf{T}^{A}]$, is given by

$$\left[\mathbf{T}^{A}\right] = \left[\mathbf{T}_e^{A}\right]\left[\mathbf{T}_a^{A}\right]\left[\mathbf{T}^{l}\right] \tag{4.9}$$

and more layers can be handled in exactly the same fashion.

4.2 Transducer Acoustic Radiation Impedance

When an ultrasonic transducer is used in an ultrasonic measurement system its acoustic port is always terminated, i.e. the output force and velocity are related to one another. For an immersion transducer radiating into a fluid, for example, we will show in Chapter 8 that for a planar piston transducer the pressure field, $p\left(\mathbf{x},\omega\right)$, on the face of the acoustic output port of the transducer is given in terms of the uniform normal velocity, $v_t\left(\omega\right)$, at that port by the Rayleigh-Sommerfeld integral:

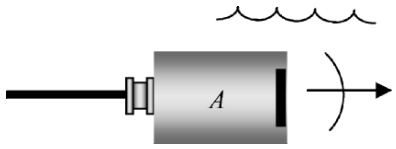

Fig. 4.8. An ultrasonic immersion transducer radiating into a fluid.

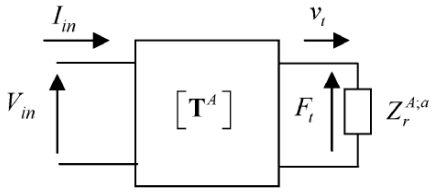

Fig. 4.9. A transducer A, whose acoustic radiation impedance is $Z_r^{A;a}$, radiating into a material and modeled as a acoustically terminated two port system.

$$p(\mathbf{x},\omega)=\frac{-i\omega\rho v_t(\omega)}{2\pi}\int_S \frac{\exp(ikr)}{r}dS(\mathbf{y}), \tag{4.10}$$

where **x** and **y** are two points on the surface, S, of the transducer face, ρ is the density of the fluid, $k=\omega/c$ is the wave number for waves propagating in the fluid whose compressional wave speed is c, and $r=|\mathbf{x}-\mathbf{y}|$ is the distance between **x** and **y**. Since the compressional force, F_t, at the transducer's output port is just the integral of this pressure, we have

$$\begin{aligned} F_t(\omega) &= \left[\frac{-i\omega\rho}{2\pi}\int_S\int_S \frac{\exp(ikr)}{r}dS(\mathbf{y})dS(\mathbf{x})\right]v_t(\omega) \\ &= Z_r^a(\omega)v_t(\omega), \end{aligned} \tag{4.11}$$

where the term in brackets in Eq. (4.11), Z_r^a, is called the *transducer radiation impedance*. The radiating transducer A of Fig. 4.8, therefore, can be represented as a terminated two port system as shown in Fig. 4.9. Greenspan [4.9] has shown that the two integrals in Eq. (4.11) can be performed for

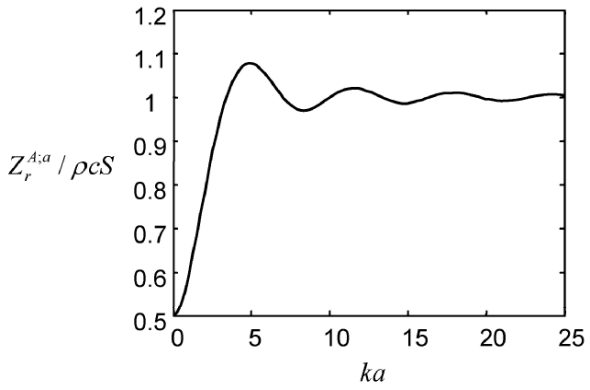

Fig. 4.10. The normalized acoustic radiation impedance of a circular, planar, piston transducer A of radius a versus the non-dimensional frequency, ka.

a circular planar piston transducer of radius a, to obtain an explicit expression for the radiation impedance given by

$$Z_r^{A;a} / \rho cS_A = 1 - \left[J_1(ka) - iS_1(ka) \right] / ka, \tag{4.12}$$

where J_1, S_1 are first order Bessel and Struve functions, respectively, and $S_A = \pi a^2$ is the area of the "active" face of the transducer at its acoustic port. Figure 4.10 shows a plot of this normalized radiation impedance versus ka, which is a non-dimensional frequency.

It can be seen from Fig. 4.10 that for approximately $ka > 10$ we can take $Z_r^a = \rho cS_A$ which is just the value of the acoustic impedance of a traveling plane wave. For most ultrasonic transducers, the ka value at the MHz frequencies used in testing is large. For example, at 5 MHz a 6.35 mm radius piston transducer radiating into water has a ka value of approximately 135. This same transducer radiating into steel would have a ka value of approximately 34. Thus, even though such ultrasonic transducers generate sound beams that are not just plane waves, their acoustic radiation impedances can generally be taken as simply as the constant value, ρcS, of a plane wave. This is true for any shaped piston transducer, not just the circular case considered by Greenspan. To see this consider Eq. (4.11) again and with $\mathbf{x}$ fixed let $dS(\mathbf{y}) = rdrd\phi'$ (see Fig. 4.11 (a)). Then the radial integration can be performed to yield

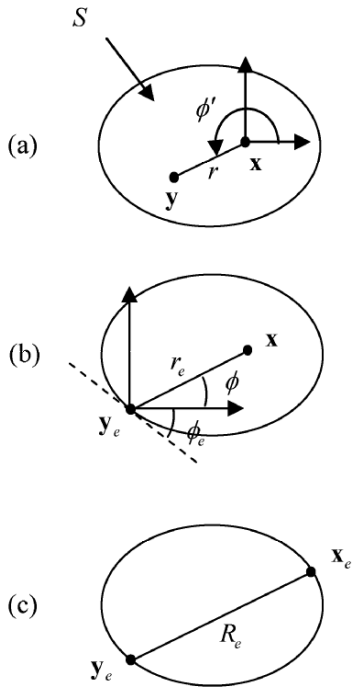

Fig. 4.11. (a) Integration over points **y** on the transducer face, and **(b)** averaging over points **x** on the transducer face, leading to **(c)** remaining integrations in terms of the distance, R_e , between points on the transducer edge.

$$\begin{aligned} F_t(\omega) &= \frac{-i\omega\rho v_t(\omega)}{2\pi}\int_S\left[\int_0^{2\pi}\int_0^{r_e}\exp(ikr)\,dr\,d\phi'\right]dS(\mathbf{x}) \\ &= \frac{\rho c v_t(\omega)}{2\pi}\int_S\left[2\pi-\int_0^{2\pi}\exp(ikr_e)\,d\phi'\right]dS(\mathbf{x}), \end{aligned} \tag{4.13}$$

where $r_e = r_e\left(\mathbf{x},\mathbf{y}_e(\phi')\right)$ is the radius from point **x** to a general point on the edge of the transducer surface, S (see Fig. 4.11 (b)). With $\mathbf{y}_e(\phi')$ fixed, we can let $dS(\mathbf{x}) = r_e dr_e d\phi$ and Eq. (4.13) becomes

$$F_t(\omega) = \rho c S v_t(\omega) - \frac{\rho c v_t(\omega)}{2\pi} \int_{-\phi_e}^{\pi-\phi_e} \int_0^{2\pi} \left[\int_0^{R_e} \exp(ikr_e) r_e dr_e \right] d\phi d\phi', \tag{4.14}$$

where R_e is shown in Fig. 4.11 (c). Performing the integral on r_e by parts, it follows that

$$\begin{aligned} \int_0^{R_e} \exp(ikr_e) r_e dr_e &= \frac{1}{ikR_e} \left[R_e^2 \exp(ikR_e) + \frac{R_e^2}{ikR_e} \left(1 - \exp(ikR_e)\right) \right] \\ &= O(1/kR_e) \end{aligned} \tag{4.15}$$

so that at high frequencies the integral in Eq. (4.14) can be neglected and we have

$$F_t(\omega) = \rho c S \, v_t(\omega) \tag{4.16}$$

4.3 Transducer Impedance and Sensitivity

Since to date there is not a practical method available to determine experimentally all the transfer matrix components of a radiating transducer, it is necessary to re-examine the terminated model of Fig. 4.9 and express it in terms of quantities that can be easily measured. In this case we can write the transfer matrix relations for a transmitting transducer *A* either in terms of the transmitted output force, F_t, or the transmitted output velocity, v_t, since

$$\begin{aligned} \begin{Bmatrix} V_{in} \\ I_{in} \end{Bmatrix} &= \begin{bmatrix} T_{11}^A & T_{12}^A \\ T_{21}^A & T_{22}^A \end{bmatrix} \begin{Bmatrix} Z_r^{A;a} v_t \\ v_t \end{Bmatrix} \\ &= \begin{bmatrix} T_{11}^A & T_{12}^A \\ T_{21}^A & T_{22}^A \end{bmatrix} \begin{Bmatrix} F_t \\ F_t / Z_r^{A;a} \end{Bmatrix}. \end{aligned} \tag{4.17}$$

The effects of this transducer on the other electrical components connected to it through its electrical port are determined by the transducer's electrical impedance, $Z_{in}^{A;e}(\omega)$, which is given by

$$Z_{in}^{A;e} = \frac{V_{in}}{I_{in}} = \frac{Z_r^{A;a} T_{11}^A + T_{12}^A}{Z_r^{A;a} T_{21}^A + T_{22}^A} \tag{4.18}$$

However, this quantity can obviously be obtained by measuring V_{in} and I_{in}, the driving voltage and current at the transducer's electrical port, respectively, when it is radiating into a material and it is not necessary to know the underlying transfer matrix components in Eq. (4.18) [4.10]. If the transducer's electrical impedance $Z_{in}^{A;e}(\omega)$ were found in this fashion by electrical measurements and if we also had characterized the pulser and cabling by the methods discussed in Chapters 2 and 3 for a given ultrasonic setup, we could then find explicitly both the voltage V_{in} and the current I_{in} at the transducer's electrical port for this setup. Thus, $Z_{in}^{A;e}(\omega)$ is all that is needed to characterize the electrical properties of the transducer in an ultrasonic measurement system. In addition, if we knew the transducer's radiation impedance, $Z_r^{A;a}$ and also obtained a measure of a quantity such as v_t / I_{in} or F_t / V_{in}, we could determine both the output force and velocity of the transducer and we would have characterized the transducer completely, i.e. both electrically and acoustically. Such quantities, which are just ratios of a transducer output to a transducer input, are called transducer transmitting sensitivities, S_{OI}, where O is an output quantity such as force or velocity, and I is an input quantity such as voltage or current, and $S_{OI} = O / I$. There are, obviously, a number of different sensitivities one could define. For example we have

$$\begin{aligned} S_{vI}^{A} &= \frac{v_t}{I_{in}} \\ S_{FI}^{A} &= \frac{F_t}{I_{in}} = Z_r^{A;a} S_{vI}^{A} \\ S_{vV}^{A} &= \frac{v_t}{V_{in}} = S_{vI}^{A} / Z_{in}^{A;e} \\ S_{FV}^{A} &= \frac{F_t}{V_{in}} = Z_r^{A;a} S_{vI}^{A} / Z_{in}^{A;e} \end{aligned} \tag{4.19}$$

We will choose to describe the transducer A in terms of its sensitivity S_{vI}^{A}. As Eq. (4.19) shows, if we also know the transducer's electrical impedance, $Z_{in}^{A;e}(\omega)$, and its acoustic radiation impedance, $Z_r^{A;a}$, we could then also obtain any of the other sensitivities listed in Eq. (4.19). From Eq. (4.17) it follows that:

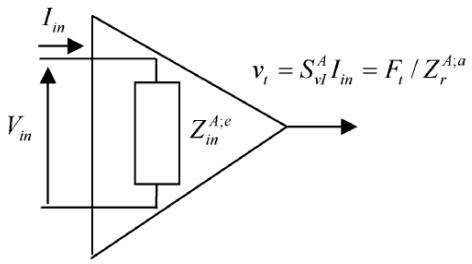

Fig. 4.12. A model of a transmitting ultrasonic transducer as an electrical impedance and an ideal "converter" that transforms the input electrical signals into the acoustic output signals.

$$S_{vI}^{A} \equiv \frac{v_t}{I_{in}} = \frac{1}{Z_r^{A;a} T_{21}^{A} + T_{22}^{A}}. \tag{4.20}$$

It will be shown in Chapter 7 that it is possible to obtain this sensitivity by direct electrical measurements of the voltage and current at the transducer's electrical port, so that there is a practical way to determine all the transducer parameters, $Z_{in}^{A;e}, S_{vI}^{A}, Z_r^{A;a}$ .Thus, we can replace the two port transfer matrix model of the transmitting transducer by the simpler model shown in Fig. 4.12, where we have represented the transducer as an electrical impedance and an ideal "converter" that transforms the input current to output velocity (or force).

4.4 The Sound Generation Process

We can combine our pulser, cabling and transducer models into a complete model of the entire sound generation process in an ultrasonic measurement system [4.10]. This generation process model is shown schematically in Fig. 4.13. We can treat this whole process as a single input, single output LTI system that is characterized by a transfer function, $t_G(\omega)$, as shown in Fig. 4.14. We will choose to write this transfer function in terms of the output force rather than the output velocity as $t_G(\omega) = F_t(\omega)/V_i(\omega)$. Since we have defined all of the elements contained in the sound generation process, we can obtain an explicit expression for this transfer function. From Fig. 4.13 we have

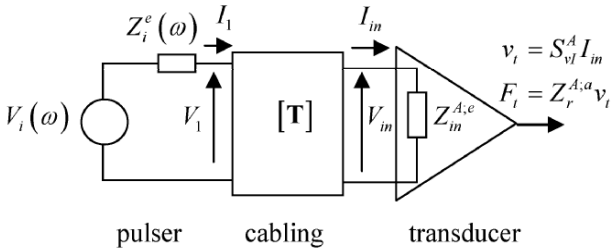

Fig. 4.13. A model of the entire sound generation process in an ultrasonic system.

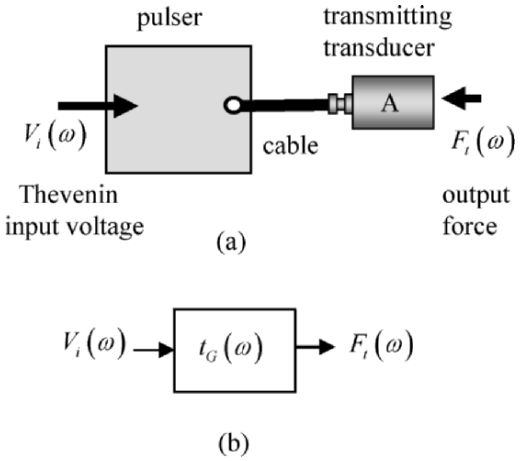

Fig. 4.14. (a) The elements in the sound generation process – the pulser, the cabling, and the transmitting transducer and **(b)** an LTI system model of the sound generation process whose transfer matrix is $t_G(\omega)$.

$$V_i - V_1 = Z_i^e I_1, \tag{4.21}$$

$$\begin{Bmatrix} V_1 \\ I_1 \end{Bmatrix} = \begin{bmatrix} T_{11} & T_{12} \\ T_{21} & T_{22} \end{bmatrix} \begin{Bmatrix} V_{in} \\ I_{in} \end{Bmatrix}, \tag{4.22}$$

$$F_t = Z_r^{A,a} S_{vI}^A I_{in}, \tag{4.23}$$

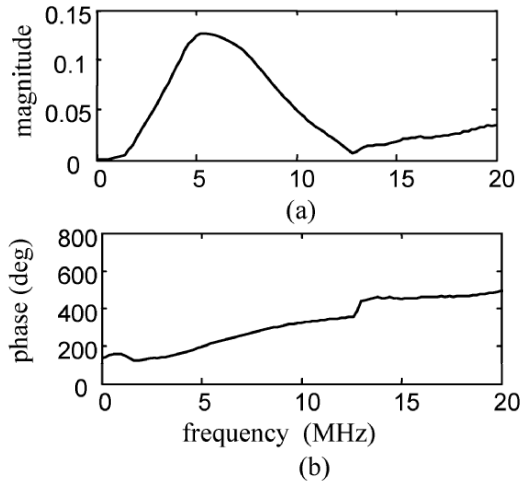

Fig. 4.15. A sound generation transfer function obtained experimentally. **(a)** Magnitude of the transfer function versus frequency and **(b)** its phase versus frequency.

$$V_{in} = Z_{in}^{A;e} I_{in}. \tag{4.24}$$

Using Eqs. (4.21 - 4.24) it is easy to show that [4.10]

$$t_G(\omega) = \frac{F_t(\omega)}{V_i(\omega)} = \frac{Z_r^{A;a} S_{vI}^A}{\left(Z_{in}^{A;e} T_{11} + T_{12}\right) + \left(Z_{in}^{A;e} T_{21} + T_{22}\right) Z_i^e}, \tag{4.25}$$

where $(T_{11}, T_{12}, T_{21}, T_{22})$ are the components of the transfer matrix, $[\mathbf{T}]$, for the cabling between the pulser and the transmitting transducer, $Z_{in}^{A;e}$ is the electrical impedance of the transmitting transducer A and S_{vI}^A is its sensitivity, and $Z_r^{A;a}$ is the acoustic radiation impedance of the transducer. With this transfer function we can model completely the effect of the pulser, the cabling and the transducer and predict the output force, $F_t(\omega)$. Figure 4.15 shows an example where the magnitude and phase of a sound generation transfer function, $t_G(\omega)$, was experimentally determined by characterizing all the components contained in Eq. (4.21). In this case the pulser was the pulser section of a Panametrics 5052 PR pulser/receiver (measured at a set of specific energy and damping settings). The cabling consisted of 1.83 m of flexible 50 ohm coaxial cable connected to a 0.61 m

fixture rod. The rod also contained internal cabling and was terminated by a right-angle adapter to which the transducer was connected. The transducer was a relatively broadband 6.35 mm diameter 5 MHz immersion transducer. The sensitivity and impedance of the transducer were obtained by the methods which will be discussed in Chapter 6.

4.5 References

4.1 Foldy LL., Primakoff H (1945) A general theory of passive linear electroacoustic transducers and the electroacoustic reciprocal theorem. J. Acoust. Soc. Am. 17: 109-120

4.2 Primakoff H, Foldy LL (1947) A general theory of passive linear electroacoustic transducers and the electroacoustic reciprocal theorem, II. J. Acoust. Soc. Am. 19: 50-58

4.3 Dang, CJ, Schmerr LW, Sedov A (2002) Modeling and measuring all the elements of an ultrasonic nondestructive evaluation system I: Modeling foundations. Research in Nondestructive Evaluation 14: 141-176

4.4 Sittig EK, (1967) Transmission parameters of thickness-driven piezoelectric transducers arranged in multilayer configurations. IEEE Trans. Sonics and Ultrasonics SU-14: 167-174

4.5 Sittig EK (1969) Effects of bonding and electrode layers on the transmission parameters of piezoelectric transducers used in ultrasonic digital delay lines. IEEE Trans. Sonics and Ultrasonics SU-16: 2-10

4.6 Mason WP (Ed.) (1964) Physical Acoustics, Vol. 1- Part A. Academic Press, New York, NY

4.7 Krimholtz R, Leedom DA, Matthaei GL (1970) New equivalent circuits for elementary piezoelectric transducers. Electronics Letters 16: 398-399

4.8 Kino GS (1987) Acoustic Waves: Devices, Imaging, and Analog Signal Processing. Prentice Hall, Englewood Cliffs, NJ

4.9 Greenspan M (1979) Piston radiator: some extensions of the theory. J. Acoust. Soc. Am. 65: 608-621

4.10 Dang CJ, Schmerr LW, Sedov A (2002) Modeling and measuring all the elements of an ultrasonic nondestructive evaluation system. II : Model-based measurements. Research in Nondestructive Evaluation 14: 177-201

4.6 Exercises

1. Equation (4.8) gave the transfer matrix for a layer in terms of the force and the velocity on both sides of an elastic layer. Consider the case where a plane compressional (P-) wave is incident on a layer, generating both

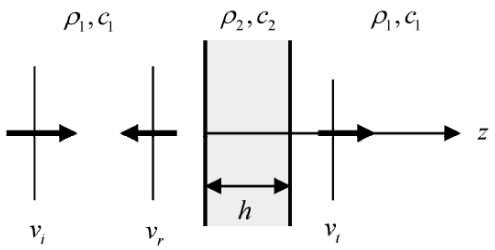

Fig. 4.16. A plane wave incident on a layer.

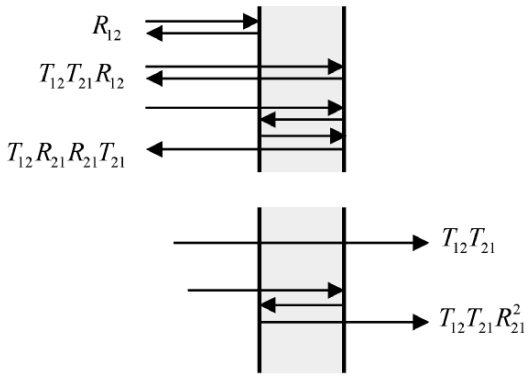

Fig. 4.17. Waves incident on a layer, showing the first few reflected and transmitted waves.

transmitted and reflected waves, as shown in Fig. 4.16. Let the velocities of these waves in their directions of propagation be given by

$$v_i = V_i \exp\left[ik_1 x\right]$$
$$v_r = V_r \exp\left[-ik_1 x\right]$$
$$v_t = V_t \exp\left[ik_1 \left(x - h\right)\right],$$

where we have written the transmitted wave in terms of the coordinate $x_2 = x - h$ since that wave only exists for $x_2 \geq 0$. Then the corresponding forces in these waves are

$$F_i = (\rho_1 c_1 S) v_i = Z_1 v_i$$
$$F_r = (\rho_1 c_1 S) v_r = Z_1 v_r$$
$$F_t = (\rho_1 c_1 S) v_t = Z_1 v_t.$$

On the sides of the layer we have $F_1 = F_i + F_r, F_2 = F_t, v_1 = V_i + V_r, v_2 = V_t$. Using Eq. (4.8) for the layer then we can obtain the reflection and transmission coefficients of the layer in the forms

$$R = \frac{F_r}{F_i} = R_{12} + \frac{R_{21} T_{12} T_{21} \exp(2ik_2 h)}{1 - R_{21}^2 \exp(2ik_2 h)}$$
$$T = \frac{F_t}{F_i} = \frac{T_{12} T_{21} \exp(ik_2 h)}{1 - R_{21}^2 \exp(2ik_2 h)},$$

where R_{ij}, T_{ij} are the plane wave reflection and transmission coefficients for a single interface going from medium *i* to medium *j* given by (see Appendix D):

$$R_{12} = -R_{21} = \frac{\rho_2 c_2 - \rho_1 c_1}{\rho_1 c_1 + \rho_2 c_2}$$
$$T_{12} = \frac{2\rho_2 c_2}{\rho_1 c_1 + \rho_2 c_2}$$
$$T_{21} = \frac{2\rho_1 c_1}{\rho_1 c_1 + \rho_2 c_2}.$$

The layer reflection and transmission coefficients (R, T) are functions of frequency because they contain all the waves that bounce back and forth in the layer and emerge into the adjacent media. To examine this behavior in frequency use MATLAB to plot the magnitude of these coefficients for 500 frequency values ranging from zero to 20 MHz for a thin (1 mm thick) aluminum plate in water. Can you explain the frequency dependent behavior of this plot?

To see the individual reflected and transmitted waves, we can expand the denominators of the (R, T) expressions and obtain

$$R = R_{12} + R_{21} T_{12} T_{21} \exp(2ik_2 h)\left\{1 + R_{21}^2 \exp(2ik_2 h) + ...\right\}$$
$$T = T_{12} T_{21} \exp(ik_2 h)\left\{1 + R_{21}^2 \exp(2ik_2 h) + ...\right\},$$

which are the first few reflected and transmitted waves as shown in Fig. 4.17. Use MATLAB to calculate the magnitude of (R,T) for just these first few terms. How do your results here compare to your previous results?